

# Diagnosis of Nonlinear Oscillatory Behavior of a Fluttering Plate with a Periodicity Ratio Approach

L. M Dai\* and X. J. Wang

<sup>1</sup> Industrial System Engineering, University of Regina,  
Regina, Saskatchewan, Canada S4S 0A2

**Abstract.** This research focuses on diagnosing the nonlinear dynamic responses of a fluttering plate excited by high-velocity air flow. An approach based on the Periodicity Ratio method is developed such that the characteristics of a nonlinear system subjected to nonperiodic excitations can be diagnosed. The governing equations of the nonlinear dynamic responses of a fluttering plate are derived and solved numerically. Eight modes of motion are used for obtaining accurate results. With the implementation of the present approach, a regular-irregular region diagram is generated for quantitatively analysing and directly visualizing the behavior of the fluttering plate with varying system parameters. Bifurcation of the plate's motion is analyzed with utilization of the regular-irregular region diagrams. The routes from regular motion to irregular motion are investigated and illustrated. Comparison is made with the diagnosing results available in the literature. The present approach demonstrates the efficiency and accuracy in the characteristic diagnosis for the fluttering plate.

**Keywords.** fluttering plate, nonlinear oscillation, aerodynamics, Periodicity Ratio, chaos, bifurcation diagram, regular-irregular diagram, nonperiodic excitation, dynamic aeroelasticity.

## Nomenclature

$D$	= plate stiffness
$E$	= modulus of elasticity
$h$	= plate thickness
$K$	= spring constant
$L$	= panel length
$M$	= Mach number
$m$	= model number
$N_x$	= in-plane force
$N_x^{(a)}$	= applied in-plane force
$p - p_\infty$	= aerodynamic pressure

$\Delta p$	= static pressure differential across the panel
$P$	= $\Delta p L^4 / Dh$
$q$	= $\rho U^2 / 2$ , dynamic pressure
$R_x$	= $N_x^{(a)} L^2 / D$
$r$	= mode number
$s$	= mode number
$t$	= time
$U_\infty$	= flow velocity
$W$	= $w / h$
$w$	= plate deflection
$\alpha$	= spring stiffness parameter
$\beta$	= $(M^2 - 1)^{1/2}$
$\lambda$	= $2q\alpha^3 / \beta D$
$\mu$	= $\rho L / \rho_m h$
$\nu$	= Poisson's ratio
$\rho$	= air density
$\rho_m$	= plate density
$\tau$	= $t(D / \rho_m h L^4)^{1/2}$

## 1 Introduction

Aeroelasticity plays an important role in the design of supersonic and hypersonic aircrafts. The fluttering or oscillation of panel structures of these aircrafts induced by the aeroelasticity would threaten the fatigue life and riding quality of the aircrafts, even the safety of the aircrafts [1]. Due to the existence of the effects of the aerodynamic, inertial and elastic forces, the dynamic behaviors of the fluttering plate become extremely complicated especially when the speed of external fluid flow increases.

Earlier investigation of flutter plate was undertaken by Dowell [2, 3]. The dynamic behaviors, including deflection, stress and frequency, under 2D and 3D, were analyzed with respect to various parameters. In the survey-type paper reported by Garrick and Reed [1], an overview of an aircraft flutter in historical retrospective is presented by the authors. The influence of maneuvering on the nonlinear response of a fluttering buckled plate on an aircraft has been studied by Sipic [4], which suggests amplitude modulation as a possible new mode of transition to chaos. The flutter phenomenon in aeroelasticity and the mathematical analysis are given by Shubov [5]. Models of fluid-structure interaction with precise mathematical formulations available are

**Corresponding author:** L. M Dai, E-mail: Limingdai@uregina.ca.

Received: 10 January 2013. Accepted: 8 February 2013.

selected and analytical results are obtained to explain flutter and its treatments. Due to the high velocity of fluid, thermal effects caused by friction have to be taken into consideration, which actually makes the problem more complicated. Enormous work could be found in this area such as [6-10].

To study the motions of fluttering plate subjected to high-velocity flow, which can be mathematically described by nonlinear differential equations of aerodynamics, the criteria for distinguishing a nonlinear motion such as chaos from regular motions are crucial. Such criteria are also important for analysing the nonlinear and regular behaviors of the system. Numerous research and great contributions have been made in investigating the characteristics of fluttering plates by researchers and engineers as mentioned above. However, based on the current literature, Lyapunov-Exponent is probably the most popular criterion used for diagnosing the characteristics of the fluttering plates. It should be noticed, nevertheless, Lyapunov-Exponent is suitable for describing whether a response of the plate is convergent or divergent. As recognized by the recent studies, a divergent response may not necessarily be chaos and the convergent ones may not all be periodic. Also, Lyapunov-Exponent cannot be used to distinguish a quasiperiodic response from the other linear or nonlinear motion of a fluttering plate [11]. Therefore, a novel approach with high accuracy and reliability and provides detailed information regarding the characteristics of the fluttering plates is in demand.

The Periodicity Ratio approach, since first introduced by Dai and Singh [12, 13] in their investigation of a Duffing's system, has demonstrated its effectiveness to characterize the behavior of a nonlinear dynamic system in addition to diagnosing chaos from regular motions and distinguishing periodic motions from nonperiodic ones [11]. By the literature available to the authors, the application of this approach so far has been limited to the cases in which the periodical external excitations are involved. For the systems of nonperiodic excitations, which are more general in the applications of real world, the implementation of the Periodicity Ratio approach has not been found. For the systems with nonperiodic excitations, the direct analogy of the techniques used in the previous research work is not suitable and a new approach needs to be developed on the basis of the Periodicity Ratio approach.

This research is to develop a method to diagnosing the characteristics of a plate subjected to nonperiodic excitations of high-velocity flow. With the method developed, the responses of the fluttering plate are to be analyzed with considerations of various varying systems parameters. A regular-irregular region diagram will be generated, by which the states of motion of the fluttering plate can be visualized and the diagram allows accurate and simultaneous examinations of regular and irregular responses of the plate. The regular-irregular region diagram generated in this research will be compared with a similar diagram existing in the literature. Bifurcation of the responses of the plate and

the transitions from one response to the others will also be studied.

## 2 The governing equation for the motion of a 2D plate

The sketch of the fluttering plate considered in this research is shown in Fig. 1. The panel, which has simply supported boundaries, is a flat thin plate with infinite length in the  $y$ -direction and length  $L$  in the  $x$ -direction. The thickness is negligible in comparing with the other geometric dimensions of the plate. The panel is subjected to a supersonic flow over the outside surface with constant velocity  $U_\infty$ . Gravity is perpendicular to the plate. The plate is induced to vibrate along the  $z$ -direction due to the loading generated by the interaction between the high-velocity flow and the plate, which is dominating and thus of great importance.

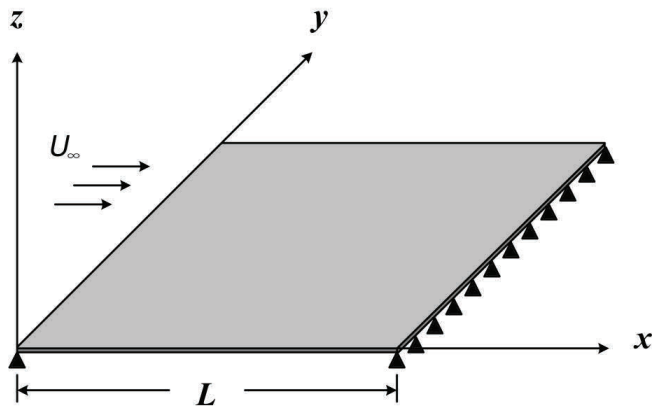


Figure 1. Panel Geometry.

To obtain the governing equations of the motion of a 2D fluttering plate, some assumptions adopted are presented first as follows:

1. The von Karman's large deflection plate theory is employed;
2. The effects of in-plane load and static pressure differential are taken into consideration;
3. The plate is undergoing cylindrical bending but no span-wise bending;
4. The material of the plate is homogeneous and isotropic;
5. With assumptions and conditions above, the motion of the fluttering plate can be considered as two-dimensional.

Based on the assumptions and conditions listed above, the governing equation for the fluttering plate can be given

as [1]:

$$D \frac{\partial^4 w}{\partial x^4} - (N_x + N_x^{(a)}) \frac{\partial^2 w}{\partial x^2} + \rho_m h \frac{\partial^2 w}{\partial t^2} + (p - p_\infty) = \Delta p \quad (1)$$

where  $w$  is the deflection of the plate,  $D$  the plate stiffness,  $\rho_m$  and  $h$  the density and thickness of the plate,  $p - p_\infty$  the aerodynamic pressure where  $p_\infty$  denotes the pressure at infinite location from the plate,  $N_x$  and  $N_x^{(a)}$  the in-plane force and applied in-plane force,  $\Delta p$  the static pressure differential across the panel.

The in-plane force is calculated as

$$N_x = \alpha E h / 2L \int_0^L (\partial w / \partial x)^2 dx \quad (2)$$

where  $E$  is the modulus of elasticity,  $L$  the panel length, and  $\alpha$  the spring stiffness parameter which is presented as

$$\alpha = KL / (KL + Eh)$$

Following the assumption of quasi-steady and supersonic theory [17], the dynamic pressure can be obtained as

$$p - p_\infty = \frac{2q}{\beta} \left[ \frac{\partial w}{\partial x} + \left( \frac{M^2 - 2}{M^2 - 1} \right) \frac{1}{U} \frac{\partial w}{\partial t} \right] \quad (3)$$

where  $q$  is dynamic pressure,  $\beta = (M^2 - 1)^{1/2}$  and  $M$  the Mach number,  $U$  the velocity of the fluid.

Applying the non-dimensionalization as follows:

$$\begin{aligned} \xi &\equiv x/L \\ \tau &\equiv t (D/\rho_m h L^4)^{1/2} \\ W &= w/h \\ \lambda &\equiv 2qL^3/\beta D \\ \mu &\equiv \rho L/\rho_m h \\ P &\equiv \Delta p L^4/Dh \end{aligned} \quad (4)$$

where  $L$  and  $h$  the length and thickness of the plate,  $D$  the plate stiffness,  $\rho_m$  the density of the plate,  $q$  is dynamic pressure and  $\Delta p$  the static pressure differential across the panel.

Substituting Eqs. (2)~(4) into (1), the non-dimensionalized governing equation can be expressed as

$$\begin{aligned} W'''' - \alpha 6(1 - \nu^2) \left[ \int_0^1 (W')^2 d\xi \right] W'' - R_x W'' + \\ + \frac{\partial^2 W}{\partial \tau^2} + \lambda \left\{ W' + \left( \frac{M^2 - 2}{M^2 - 1} \right) \left( \frac{\mu}{\beta \lambda} \right)^{1/2} \frac{\partial W}{\partial \tau} \right\} = P \end{aligned} \quad (5)$$

where  $\alpha$  is the spring stiffness parameter,  $\nu$  the Poisson's ratio and  $R_x = N_x^{(a)} L^2/D$ .

For large Mach number,  $M \gg 1$ , the simplified relationship can be applied which reads

$$\left[ \frac{M^2 - 2}{M^2 - 1} \right]^2 \frac{\mu}{\beta} \rightarrow \frac{\mu}{M} \quad (6)$$

where  $\mu$  is the viscosity of the fluid.

Following the Galerkin Method [15], for simply supported plate, the non-dimensional displacement  $W(\xi, \tau)$  can be expressed by the basis functions as

$$W(\xi, \tau) = \sum_{m=1}^{\infty} a_m(\tau) \cdot \sin m\pi\xi \quad (7)$$

where  $a_m$  represents the temporal variation modes.

For the sake of clarification and simplicity, in the following, Eq. (6) will be used. Substituting Eqs. (6) and (7) into Eq. (5), then Eq. (5) can be rewritten as:

$$\begin{aligned} \sum a_m(m\pi)^4 \sin m\pi\xi + \alpha 6(1 - \nu^2) \times \\ \left[ \sum_r a_r^2 \frac{(r\pi)^2}{2} \right] \sum_m a_m(m\pi)^2 \sin m\pi\xi + \\ + R_x \sum_m a_m(m\pi)^2 \sin m\pi\xi + \sum_m \frac{d^2 a_m}{d\tau^2} \sin m\pi\xi + \\ + \lambda \left[ \sum_m a_m(m\pi) \cos m\pi\xi + \left( \frac{\mu}{M\lambda} \right)^{1/2} \sum_m \frac{da_m}{d\tau} \sin m\pi\xi \right] = \\ = P \end{aligned} \quad (8)$$

By multiplying Eq. (8) by  $\sin(m\pi\xi)$  and integrating over the length of the panel, Eq. (8) can be reduced into a set of ordinary differential equations.

$$\begin{aligned} a_s \frac{(s\pi)^4}{2} + \alpha 6(1 - \nu^2) \left[ \sum_r a_r^2 \frac{(r\pi)^2}{2} \right] a_s \frac{(s\pi)^2}{2} + \\ + R_x a_s \frac{(s\pi)^2}{2} + \frac{d^2 a_s}{d\tau^2} \frac{1}{2} + \lambda \left\{ \sum_m \frac{sm}{s^2 - m^2} \times \right. \\ \left. [1 - (-1)^{s+m}] a_m + \frac{1}{2} \left( \frac{\mu}{M\lambda} \right)^{1/2} \frac{da_s}{d\tau} \right\} = P \frac{[1 - (-1)^s]}{s\pi}, \\ s = 1, \dots, \infty \end{aligned} \quad (9)$$

Eq. (9) is comprised of a coupled set of ordinary, nonlinear differential equations with respect to time. For such a complex nonlinear system, one may have to rely on numerical solutions as the solutions of analytical form are very difficult to obtain if not possible. In this research, the 4<sup>th</sup> order Runge-Kutta method is employed for pursuing numerical solutions and performing numerical analysis [16]. It

has been reported in [1] that to obtain accurate solutions, at least 4 modes must be used. When the in-plane or static pressure loading produces larger tension in the plate, more modes would be taken into consideration. In this paper, under the range of parameters applied, all the calculations are performed using eight modes. The accuracy of the numerical solutions is demonstrated against those obtained in [1] and good agreement is obtained as shown in Fig. 2.

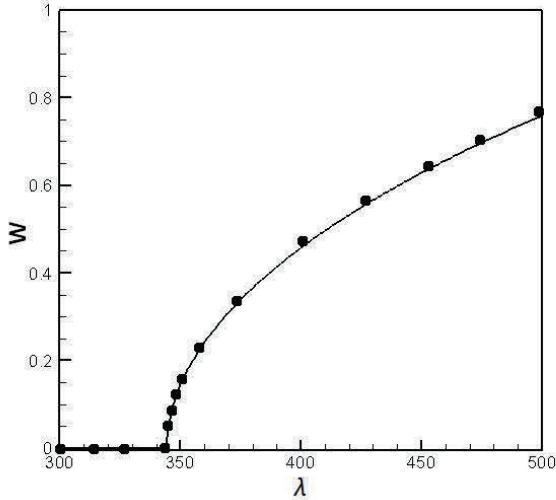


**Figure 2.** The plate deflection against  $\lambda$  (the continuous line is obtained by the author, the dots by [1]).

In Fig. 3, the deflection shapes under different values of  $R_x$  are presented. The amplitude of deflection becomes greater as  $R_x$  decreases. Also, analysis of Figure. 1 indicates the maximum deflection occurs at about  $\xi = 0.75$ . The following calculation will be implemented at this point. It is obvious that there are nonlinear effects other than the one shown above. For Mach number of the order of one, both the aerodynamic nonlinearities and the nonlinear structural effect of large curvature play the key role, while other nonlinear effects are unlikely to be of any importance [1]. As a result, the following work will mainly focus on two parameters, namely,  $R_x$  and  $\lambda$ .

### 3 Nonlinear behavior characterization with periodicity ratio approach

#### 3.1 Regular-irregular region diagrams corresponding to varying parameters of the fluttering plate

The Periodicity Ratio approach, a criterion for distinguishing between periodic, quasiperiodic and chaotic response of a nonlinear system, was first introduced by Dai and Singh [12] in their investigation of a Duffing system. This single valued criterion is applied based on Poincare maps that for a

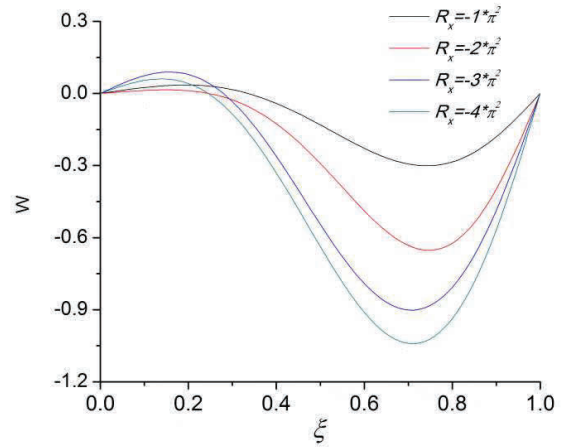


**Figure 3.** Panel Deflection Shape ( $\mu/M = 0.01, \lambda = 200, p = 0.0$ ).

periodic motion, the visible points demonstrating motion of the same period in a Poincare map will eventually overlap each other given a large enough period of time. However, for a chaotic or quasiperiodic motion, overlapping points range from a few to none in the Poincare map due to the fact that they are randomly spread over the corresponding phase plane. From this point of view, a criterion for analyzing the dynamic behaviors can be applied to consider the overlapping points with the total number of points in the Poincare map. To do this, a parameter called periodicity ratio is defined as:

$$\gamma = \lim_{n \rightarrow \infty} \frac{NOP}{n} \quad (10)$$

In Eq. (10),  $NOP$  is denoted as the total number of periodic points which are overlapping points and  $n$  represents the number of all the points forming the Poincare map.  $NOP$  can be obtained by the formula shown below:

$$NOP = \zeta(1) + \sum_{k=2}^n \zeta(k) \cdot P \left( \prod_{l=1}^{k-1} \{X_{kl} + \dot{X}_{kl}\} \right) \quad (11)$$

In the equation above,  $\zeta(k)$  represents the number of points overlapping the  $k$ th point in the Poincare map, and  $\prod$  is the symbol for multiplication.  $X_{kl}$ ,  $\dot{X}_{kl}$  and  $P(z)$  are functions expressed as

$$X_{kl} = |X(\tau_0 + kT) - X(\tau_0 + lT)| \quad (12)$$

$$\dot{X}_{kl} = |\dot{X}(\tau_0 + kT) - \dot{X}(\tau_0 + lT)| \quad (13)$$

$$P(z) = \begin{cases} 0 & \text{if } z = 0 \\ 1 & \text{if } z \neq 0 \end{cases} \quad (14)$$

As mentioned above, if the motion is pure periodic, all the points in Poincare map will be overlapping points and they would appear periodically so that  $\gamma$  will equal one. On the other hand, if  $\gamma$  is very small or even zero, the motion clearly belongs to quasiperiodic or chaotic motion. When  $\gamma$  falls between 0 and 1, the motion is a mixture of both periodic and non-periodic motions. It is obvious that  $\gamma$  can be tread as a criterion of characterizing the dynamic behaviors for regular and irregular motions. Its effectiveness and accuracy have been proved in [14] considering Duffing equation.

However, by now the application of Periodicity Ratio method is limited only to application on the dynamic systems of periodical external excitations. Direct employment of Periodicity Ratio method to diagnose the fluttering plate, whose motions are excited by the nonperiodical interaction between high-velocity flow and plate, would give inaccurate results and thus be unavailable. Therefore, when the periodicity ratio method is applied to the specific case of the fluttering plate, the difficulties caused by nonperiodical excitations must be overcome first, which causes a difficulty in the construction of the Poincare map. In [15], one way to construct the Poincare map for such a case is introduced when the points in Poincare map corresponding to the nondimensional velocity  $\dot{W} = 0$  are selected.  $\dot{W} = 0$  indicates the maximum deflection amplitude of the plate. Once we find the way to draw the Poincare map, the periodicity ratio method can be easily performed.

Eq. (11) is then modified as:

$$NOP = \zeta(1) + \sum_{k=2}^n \zeta(k) \cdot P \left( \prod_{l=1}^{k-1} W_{kl} \right) \quad (15)$$

where

$$W_{kl} = |W_k - W_l|. \quad (16)$$

$W_k$  represents the  $k$ th point on Poincare map, in considering that  $W_k$  is taken in a Poincare section where the nondimensional displacement is the maximum.

However, to obtain the numerical solution, the point corresponding to  $\dot{W} = 0$  cannot be calculated exactly since the numerical solution for the governing equation can only be discretized and the fixed time step is applied when we use the 4<sup>th</sup> order Runge-Kutta method. As a result, a process is required to determine the approximate maximum deflection points, which is presented as follows:

Suppose the series  $W_n = W(t_n)$  are the numerical solutions, where subscript  $n$  represents  $1, 2, \dots, \infty$ . The values which indicate the maximum deflection are chosen when

$$|W_n > W_{n-1}| \text{ and } |W_n > W_{n+1}|. \quad (17)$$

To illustrate this clearly, a small portion of the wave diagram of the system is presented as shown in Fig. 4. The

dots in this figure represent the points selected for Poincare map. As can be observed from Fig. 4, the motion is periodic. The points in this figure can be grouped into four sets and the points in each set have identical  $W$  values. Therefore, there are only four sets of points visible and the others are overlapped by these four points. This should be the case no matter how large the time range is considered, provided that the system maintains the stable periodic motion.

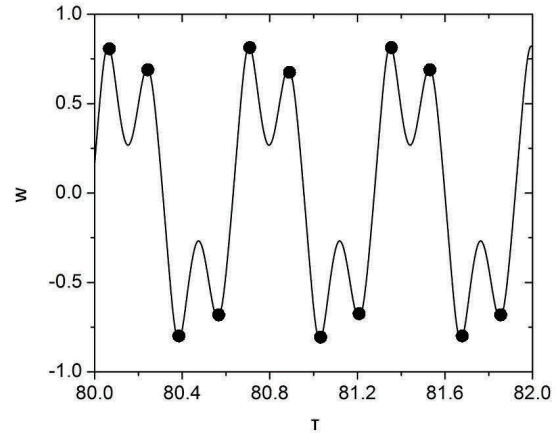


**Figure 4.** Wave diagram and points corresponding to Poincare map.

In analysing the complex behavior of a nonlinear system such as the fluttering plate under the excitation of high speed fluid, it is practically convenient to have a diagram in which the regions illustrating regular and irregular responses of the system can be plotted corresponding varying system parameters. Specifically, with the diagram, the irregular responses of a nonlinear system can be directly visualized in reflecting the system parameters. To construct such a diagram to show regular and irregular regions,  $R_x$  and  $\lambda$  are taken into consideration as the varying parameters. The diagram is known as the region diagram hereafter. Corresponding to the two parameters a region diagram is plotted as shown in Fig. 4. Though the two system parameters are used for the diagram, however, the other system parameters can be considered if so desired.

In Fig. 4, the red color represents regular region, while the blue mean irregular region. Other colors represent the motion between the stable and unstable motions. This figure provides a global picture of the properties of the motion of the plate. It can be seen that most of the region of the graph consists of stable points.

The region diagram Fig. 5 compares well with the results reported [1] except in two areas. As mentioned above, the periodicity ratio is determined by the characteristics of overlapping points, which are generally distributed into several sets of overlapping points. By summing up the sets' number obtained in computing periodicity ratio, the regular

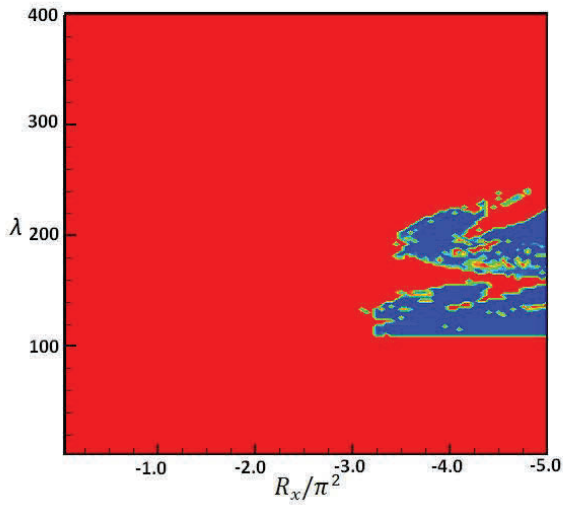


Figure 5. Region Diagram.

motion can be easily distinguished as stable, simple harmonic and double periodical motions etc., shown as Fig. 6.

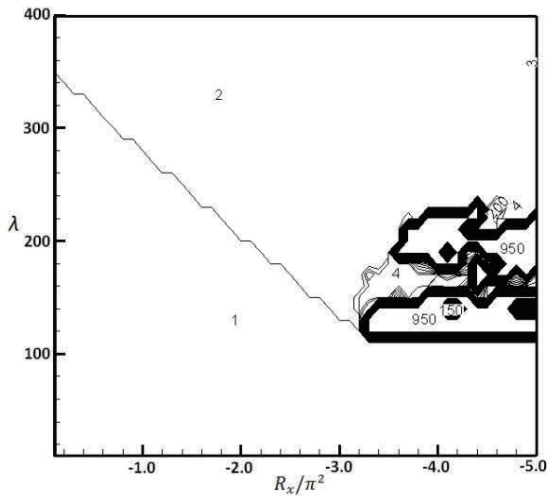


Figure 6. Contour of the sets of overlapping points.

In comparing with the corresponding diagram in [1] and that in Fig. 6, the first difference is about the point where  $R_x/\pi^2 = -5$  and  $\lambda = 350$ . According to [1], the motion at this point is simple harmonic. However, based on the PR method, the number of set is more than 2, which actually implies a complicated periodical motion. As illustrated by the wave trajectory in Fig. 7. For this point, the motion is periodic but not simple harmonic.

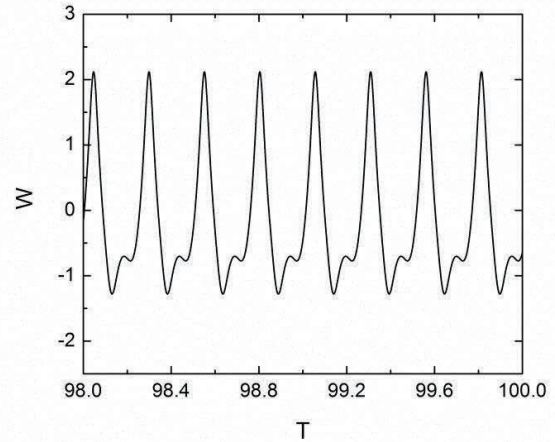


Figure 7. Wava Diagram ( $R_x/\pi^2 = -5, \lambda = 350$ ).

Another area shows difference from that of [1] is the region demonstrated as periodic but not simple harmonic in [1]. The motion in this area consists not only complicated periodical motions, but also irregular motions according to Periodicity-Ratio obtained. This is the motion corresponding to  $R_x/\pi^2 = -4$  and  $\lambda = 200$ . The corresponding phase trajectory is presented in Fig. 8. It is evident that the motion in this case is chaotic but not periodic or regular.

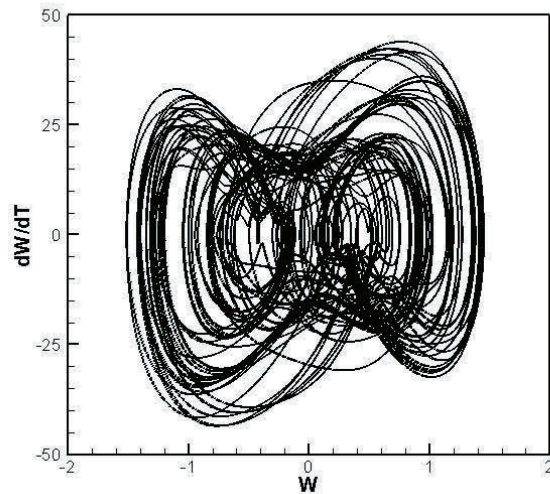


Figure 8. Phase trajectory of chaotic motion ( $R_x/\pi^2 = -4, \lambda = 200$ ).

In fact, the patterns of motion are different from region to region. Region with one type of motion can be easily distinguished from the other region in which the motion is different with implementation of PR approach. Four types of motion within the range of the parameters are considered. As illustrated in Fig. 9, dark blue represents flat motion,

green represents buckled motion, yellow denotes regular oscillation and red is irregular oscillations. Three patterns of stable responses of the system are chosen from Fig. 9 and illustrated by the wave diagrams and phase trajectories in Figs. 10–12.

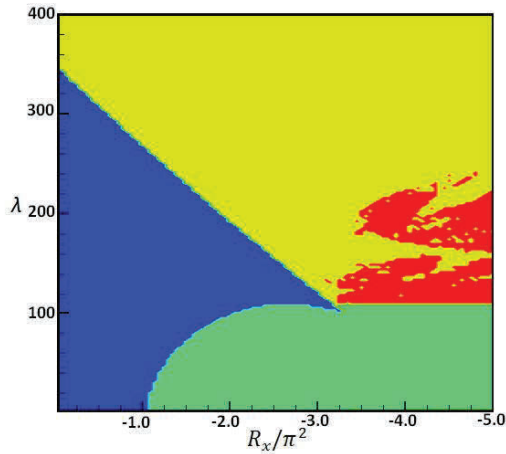


Figure 9. Patterns of Motions.

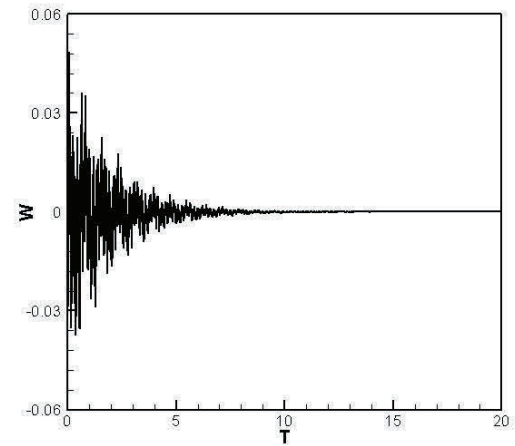
From the figures listed above, it can be recognized that among the stable motions, some reach a final static point as demonstrated in Figs. 10 and 11, and the others tend to converge to a simple harmonic oscillation as shown in Fig. 12.

3.2 Transition from a regular point to irregular points

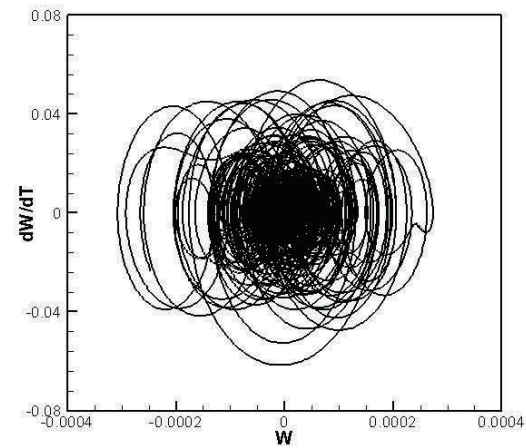
As mentioned above, the regular and irregular region diagrams can be conveniently constructed by implementing the periodicity ratio method and then be applied to analyze the dynamic behavior of the fluttering plate. Also, the diagram can be used to capture the routes from regular motions to irregular motions. Irregular regions are surrounded by or bounded with regular region, which is observed through the regular-irregular region diagram. By changing either one or both of the control parameters in the system, the routes from regular motion to irregular motions can be identified.

As shown in Fig. 5, along a fixed horizontal line  $\lambda = 200$ , motions of the system vary from stable to simple harmonic, then to irregular. This variation of motion is illustrated in the bifurcation diagram of Fig. 13. Starting from  $R_x = 0$ , a dynamically stable and static motion is obtained for which the corresponding Poincare map consists of only one set of points over the selected time range. As the value of  $R_x$  decreases, bifurcation of the system occurs. When  $R_x/\pi^2$  reaches approximately  $-1.85$ , a periodic oscillation is observed. Irregular motion appears when  $R_x/\pi^2$  is less than  $-3.38$ .

Similarly, the transition from irregular motion to regular motion along the vertical line  $R_x/\pi^2 = -4$  is also demonstrated in Fig. 5. The corresponding variation is depicted



Wave Diagram (flat)



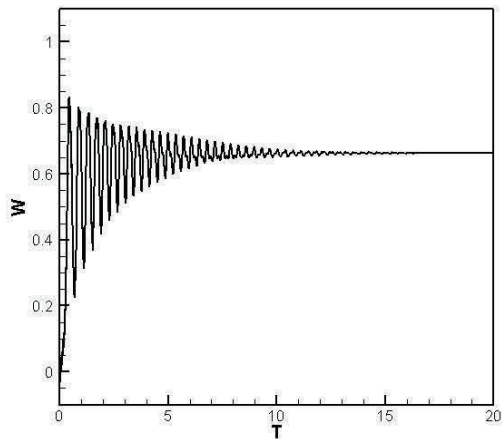
Phase Trajectory

Figure 10. Flat Motion ( $R_x/\pi^2 = -1, \lambda = 100$ ).

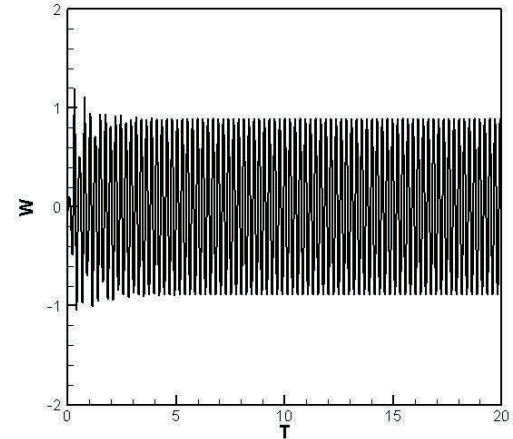
in the bifurcation diagram of Fig. 14, where the motion becomes irregular when  $\lambda$  exceeds 114 and returns to regular after  $\lambda$  surpasses 225.

4 Conclusion

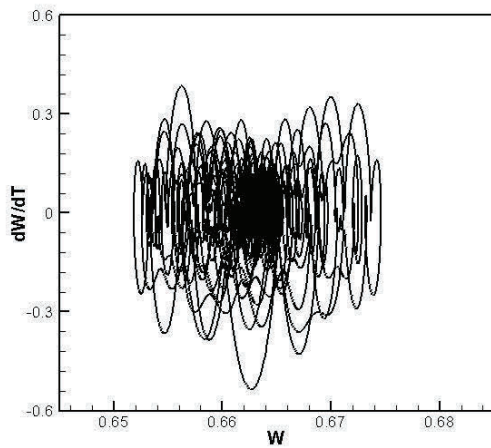
The dynamic behavior of a fluttering plate can be very complex. The model used in this research describes a nonlinear plate system subjected to the nonlinear excitations of high speed fluid. In order to quantitatively analyze the characteristics of such a complex system, a new approach based on the Periodicity Ratio (PR) method is introduced. Most of the studies on the nonlinear behavior with employment of PR method are for the systems subjected to periodic excitations. The present approach constructs the Poincare maps with considerations of the maximum deflections of



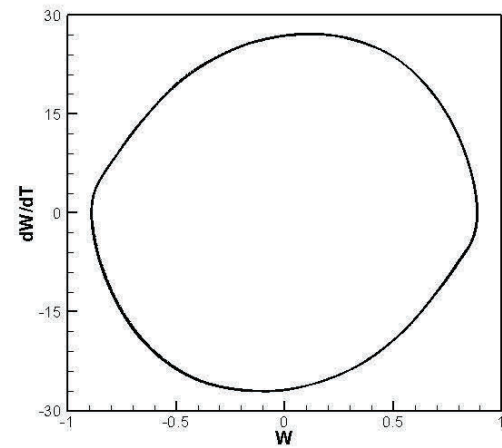
Wave Diagram (bucked)



Wave Diagram (harmonic)



Phase Trajectory



Phase Trajectory

**Figure 11.** Buckled and stable motion ( $R_x/\pi^2 = -3, \lambda = 50$ ).

**Figure 12.** Limit Cycle Oscillation ( $R_x/\pi^2 = -3, \lambda = 300$ ).

the plate. The Poincare maps such constructed therefore the PR values determined based on the Poincare sections better reflect the responses of the nonlinear fluttering plate and show great advantage in analyzing the behavior of the plate system.

With employment of the present approach, regular and irregular responses of the fluttering plate subjected to non-periodical external excitations can be efficiently studied. A regular-irregular region diagram for the plate system is plotted with the results obtained. In comparing with the published results in the literature, the results and the regular-irregular region diagram of the present research reflect more accurately and completely the behavior of the plate system. Some of incorrect results in the previous publications are also identified. Yet, with employment of the present approach, no single plot such as phase diagram and wav form

diagrams is needed in constructing the regular-irregular region diagram. Although the regular-irregular region diagram presented considers the two parameters of the system, the region diagrams for the other system parameters can be easily constructed with the same approach.

As demonstrated in the research, the present approach show high efficiency in analyzing and directly visualizing the responses of a complex nonlinear system. Pattern of the routes to irregular motion may also be conveniently investigated with the present approach, such as the route of buckling  $\rightarrow$  periodic oscillations  $\rightarrow$  irregular motions. The present research may provide a practically sound guidance to the researchers and engineers in identifying the characteristics of the nonlinear fluttering plates and thus avoiding the design that may lead to unwanted responses.

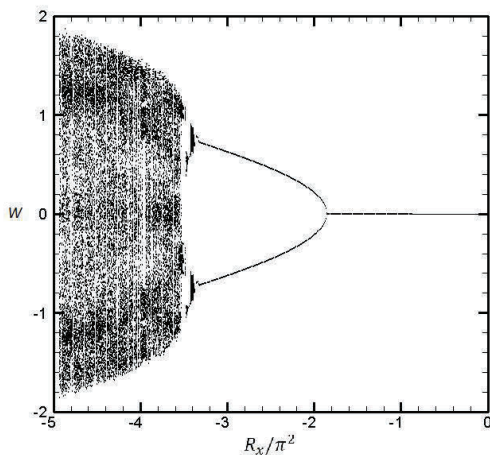


Figure 13. Bifurcation Diagram ( $\lambda = 200$ ).

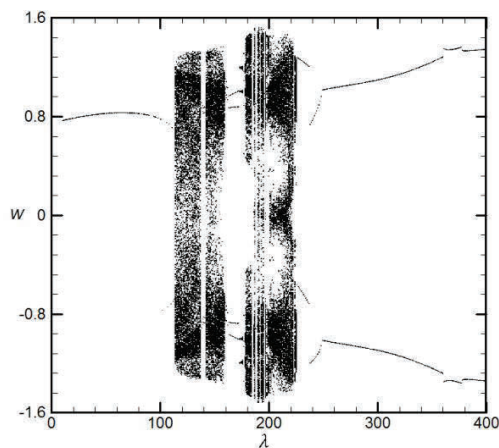


Figure 14. Bifurcation Diagram ( $R_x/\pi^2 = -4$ ).

## References

- [1] Garrick, E. I., and Reed, W. H., [1981], "Historical development of aircraft flutter," *J. Aircr.*, **18**(11), 897-912.
- [2] Dowell, E. H., [1966], "Nonlinear oscillations of a fluttering plate," *AIAA Journal* **4**(7), 1267-1275.
- [3] Dowell, E. H., [1967], "Nonlinear oscillations of a fluttering plate II," *AIAA Journal* **5**(10), 1856-1862.
- [4] Sipic, S. R., [1990], "The chaotic response of a fluttering panel: the influence of maneuvering," *Nonlinear Dynamics* **1**(3), 243-264.
- [5] Shubov, M. A., [2006], "Flutter phenomenon in aeroelasticity and its mathematical analysis," *Journal of Aerospace Engineering* **19**(1), 1-12.
- [6] Dowell, E. H., and Ventres, C. S., [1970], "Comparison of theory and experiment for nonlinear flutter of loaded plates," *AIAA Journal* **8**(11), 2022-2030.
- [7] Librescu, L., Marzocca, P., and Silva, W. A., [2004], "Linear/Nonlinear supersonic panel flutter in a high-temperature field," *Journal of Aircraft* **41**(4), 918-924.
- [8] Li, K. L., Zhang, J. Z., and Lei, P. F., [2010], "Simulation and nonlinear analysis of panel flutter with thermal effects in supersonic flow," *Dynamical Systems* (Springer, New York), pp. 61-76.
- [9] Schaeffer, H. G., and Heard, W. L., [1965], "Flutter of a flat panel subjected to a nonlinear temperature distribution," *AIAA Journal* **3**(10), 1918-1923.
- [10] Xue, D. Y., and Mei, C., [1993], "Finite element nonlinear panel flutter with arbitrary temperatures in supersonic flow," *AIAA Journal* **31**(1), 154-162.
- [11] Dai, L., and Wang, G., [2008], "Implementation of periodicity ratio in analyzing nonlinear dynamic systems: a comparison with Lyapunov Exponent," *Journal of computational and nonlinear dynamics*. Vol. 3,(011006)1-9.
- [12] Dai, L., and Singh, M. C., [1995], "periodicity ratio in diagnosing chaotic vibrations," *15<sup>th</sup> Canadian congress of Applied Mechanics 1*, 390-391.
- [13] Dai, L., and Singh, M. C., [1998], "Periodic, Quasiperiodic and Chaotic Behavior of a Driven Froude Pendulum," *International Journal for Non-Linear Mechanics*, **33**(1), 947-965.
- [14] Hosseini, M., and Fazelzadeh, S. A., [2010], "Aerothermoelastic Posting-Critical and Vibration Analysis of Temperature-Dependent Functionally Graded Panels," *Journal of Thermal Stress*, 33: 1188-1212.
- [15] Donea, J., [1984], "A Taylor-Galerkin method for convective transport problems," *International Journal for Numerical Methods in Engineering* **20**(1), 101-119.
- [16] Ascher, U. M., and Petzold, L. R., [1998], "Computer Methods for Ordinary Differential Equations and Differential-Algebraic Equations", *Philadelphia: Society for Industrial and Applied Mathematics*, ISBN 978-0-89871-412-8.
- [17] Dowell, E. H., [1996], "Nonlinear Oscillations of a Fluttering Plate", *AIAA Journal* **4**(7), 1267-1275.
- [18] Dowell, E. H., and Voss, H. M., [1965], "Experimental and theoretical panel flutter studies in the Mach number range 1.0 to 5.0," *AIAA Journal* **3**(12), 2292-2304.
- [19] Pourtakdoust, S. H., and Fazelzadeh, S. A., [2003], "Chaotic Analysis of Nonlinear Viscoelastic Panel Flutter in Supersonic Flow," *Nonlin. Dynam.* **4**(32), 387-404.
- [20] Stoker, J. J., [1950], "Nonlinear Vibrations," Wiley-Interscience, New York.

